Catal Lett (2007) 119:64–71
DOI 10.1007/s10562-007-9190-x

Preparation of Vanadium Phosphate Catalysts from $VOPO_4 \cdot 2H_2O$: Effect of Microwave Irradiation on Morphology and Catalytic Property

Y. H. Taufiq-Yap · A. A. Rownaghi · M. Z. Hussein · R. Irmawati

Received: 19 March 2007 / Accepted: 26 June 2007 / Published online: 20 July 2007

Abstract The present work addresses the influence of microwave irradiation on undoped and doped vanadium phosphate catalysts. These catalysts were prepared via $VOPO_4 \cdot 2H_2O$. The catalyst's precursors' $VOHPO_4 \cdot 0.5H_2O$ were subjected to microwave irradiation and comparison was made with the conventional heating. The interaction of these complex materials with microwave and the addition of several doponts (Nb, Bi, Co, Mo) provide interesting improvements in catalyst preparation found to be a faster, develop higher surface area, higher activity and selectivity for the oxidation of *n*-butane to maleic anhydride. All the catalysts were characterized by using a combination of powder XRD, H_2-TPR, BET surface area and SEM.

Keywords Vanadium phosphate · Microwave heating · *n*-butane oxidation · Maleic anhydride

1 Introduction

The selective oxidation of *n*-butane continues to receive considerable research attention. In this respect vanadium phosphate catalyst has been extensively investigated and to date it represent the sole example of a commercial catalyst for the selective oxidation of an alkane [1]. The catalytic performance of vanadium phosphates depends on the method of preparation of the catalyst precursor, $VOHPO_4 \cdot 0.5H_2O$ [2–4], and the reaction conditions utilized for the activation in *n*-butane/air to form the final catalyst [2, 3]. The active catalyst comprises $(VO)_2P_2O_7$ in combination with some V^{5+} phosphates, typically α_{II}- and δ-$VOPO_4$, and the transformation of the precursor to the final catalyst is topotactic [4]. Hence, the preparation route and the precursor's morphology is of importance in determining the eventual catalyst morphology and the performance following activation.

In general, for the preparation of $VOHPO_4 \cdot 0.5H_2O$, V_2O_5 is used as a source of vanadium and H_3PO_4 is used as a source of phosphorus. Hence, a reducing agent is required to synthesis the V^{4+} precursor phase and a broad range of reducing agents and solvents have been employed [2–11]. Early studies tended to use water as solvent and in this case hydrochloric acid was utilized as reducing agent. This method prepares low area materials that have $VO(HPO_4)_2$ as an impurity [4]. A major innovation was the introduction of an alcohol, typically isobutanol, as both the solvent and the reducing agent [5], and this method tends to give much higher surface area materials without the presence of impurities.

Despite plentiful studies worldwide, progress in this field has been hampered by low *n*-butane conversion and serious catalyst deactivation due to coke formation. It is well known that the preparation method of catalyst can affect the channel structure, the acid site density, and the oxidation state and location of the vanadium species. These factors are recognized to affect the catalytic performance of *n*-butane conversion. Thus, this leads to the investigation of new preparation method and to the further optimization of catalyst performance. Microwave heating has been shown to be a promising technique for catalyst preparation because of its heating characteristic [12, 13].

Y. H. Taufiq-Yap (✉) · A. A. Rownaghi · M. Z. Hussein · R. Irmawati
Putra Laboratory for Catalysis Science and Technology, Department of Chemistry, Faculty of Science, Universiti Putra Malaysia, 43400 UPM Serdang, Selangor, Malaysia
e-mail: yap@fsas.upm.edu.my

In the present work, we would like to report the effect of microwave irradiation on undoped and several-doped VPO catalyst such as (Nb, Mo, Co, Bi) synthesized via dihydrate method in order to obtain information linking catalytic behavior of the solids with their physicochemical properties. These catalysts were characterized by using a combination of powder XRD, H_2-TPR, BET surface area, and SEM.

2 Experimental

2.1 Catalysts Preparation

The preparation of vanadyl hydrogen phosphate precursor ($VOHPO_4 \cdot 0.5H_2O$) via reduction of $VOPO_4 \cdot 2H_2O$ phase was adopted from the open literature [4] and is detailed as follow; through the dihydrate route (VPD), a two-step preparation procedures involved with $VOPO_4 \cdot 2H_2O$ as an intermediate before obtaining the precursor ($VOHPO_4 \cdot 0.5H_2O$). $VOPO_4 \cdot 2H_2O$ was first prepared by employing the reaction of vanadium (V) pentoxide, V_2O_5 (12.0 g from Fisher Chemicals) with *ortho*-phosphoric acid 85% (115 g, from Fisher). This mixture in water (24 mL H_2O/g solid) was refluxed with rapid stirring for 24 h before obtaining yellow product. Then the resulting mixture (yellowish colored) was recovered by filtration and washed with hot distilled water (100 mL) and acetone (100 mL). The solid was then divided into two parts. One part was heated for 2 min by microwave method (denoted VPO_{H1}). The heating conditions were at 2450 MHz with an output power of 160 W. The other part was heated for 16 h at 393 K under atmospheric condition in an oven (denoted VPO_{H2}). Both specimens were confirmed as $VOPO_4 \cdot 2H_2O$ by XRD. The second step of preparation was preceded as $VOPO_4 \cdot 2H_2O$ was heated again with isobutyl alcohol (1 g/20 mL from BDH Chemicals) and definite amount of dopants: Nb_2O_5, $((NH_4)_6Mo_7O_{24}) \cdot 4H_2O$, $CoN_2O_6 \cdot 6H_2O$ or $Bi(NO_3)_3 \cdot 5H_2O$ maintained under reflux with constant stirring for 21 h. After the reduction reaction is completed, the blue solid phase was recovered by filtration and washed with hot distilled water (100 mL) and acetone (100 mL) and dried with microwave heating and oven for 2 min and 12 h respectively.

The obtained blue solid was then heated for 2 min in microwave (MW) as mentioned above. The other was heated in an oven under atmosphere condition (conventional heating, CH). All the dried precursors were calcined in a flow of *n*-butane/air mixture at 733 K for 6 h. The undoped and doped catalysts heated by microwave were designated VPOA1, VPOB1, VPOC1, VPOD1 and VPOE1, and the catalysts with the same composition heated in conventional method were designated VPOA2, VPOB2, VPOC2, VPOD2 and VPOE2.

2.2 Catalysts Characterization

The XRD analyses were carried out using a Shimadzu diffractometer model XRD 6000 employing CuK_α radiation to generate diffraction patterns from powder crystalline samples at ambient temperature.

The total surface area and porosity of the catalysts were measured by the BET (Brunauer–Emmer–Teller) method using nitrogen adsorption at 77 K. This was done by the Sorptomatic 1990 series nitrogen adsorption/desorption analyzer.

A Jeol JSM-6400 scanning electron microscope (SEM) was used to obtain topographical information from the catalysts.

TPR (temperature-programmed reduction) analysis was done by using a ThermoFinnigan TPDRO 1110 apparatus utilizing a thermal conductivity detector (TCD). TPRs were performed for each material using a quartz reactor tube (4 mm i.d.), in which a ~25 mg sample was mounted on loosely packed quartz wool. The sample was heated at 10 °C/min up to 900 °C under 25 mL/min flow of a 5% mixture of H_2 in Ar.

The average oxidation state of vanadium was determined by the method described by Niwa and Murakami [14].

2.3 Catalytic Test

The oxidation of *n*-butane to maleic anhydride was carried out in a fixed-bed flow microreactor containing a standard mass of catalyst (0.25 g) at 673 K with GHSV of 2400 h^{-1}. Prior to use, the catalysts were pelleted and sieved to give particles (250–300 μm in diameter). *n*-Butane and air were fed to the reactor via calibrated mass flow controllers to give a feedstock composition of 1.7% *n*-butane in air. The products were fed via heated lines to an on-line gas chromatography for product analysis. The reactor comprised a stainless steel tube with the catalyst held in place by plugs of quartz wool. A thermocouple was located in the center of the catalyst bed and temperature control was typically ±1 K. Carbon mass balances of ≥97% were typically observed.

3 Results and Discussion

3.1 X-ray Diffraction (XRD)

The structural effect of microwave heating on the dihydrate ($VOPO_4 \cdot 2H_2O$) is shown in Fig. 1. XRD diffractograms of both vanadyl phosphate hydrate gave similar pattern with peaks at $2\theta = 11.89$, 23.93 and 28.71°. However, microwave irradiated sample shows higher crystalline

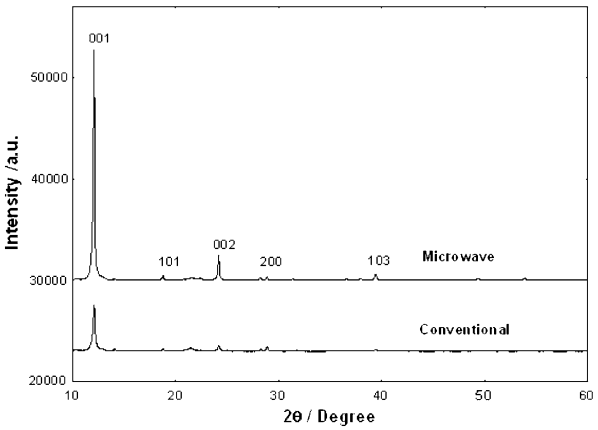

Fig. 1 XRD Patterns of microwave and conventional heated $VOPO_4$ $2H_2O$ dihydrate

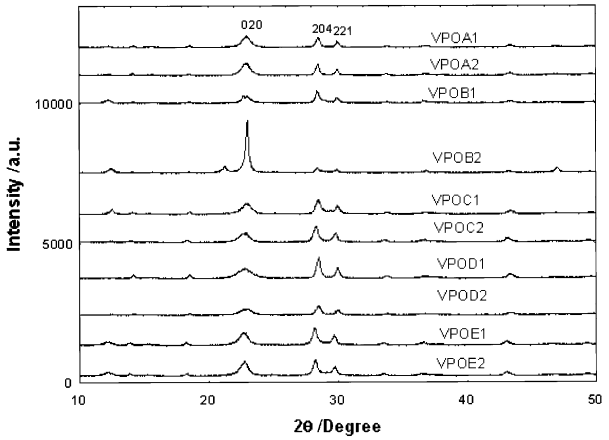

Fig. 3 XRD Patterns of microwave and conventional heated $(VO)_2P_2O_7$ catalysts

structure, which indicated by the high intensity of the peaks. XRD patterns of all hemihydrates precursors (Fig. 2) are identical to $VOHPO_4 \cdot 0.5H_2O$ with peaks at 2θ = 15.48, 19.56, 24.14, 27.00 and 30.34°. The preparation method and different additives affected on the d-spacing of [001] plane of the hemihydrate. It is known that the (001) plane of $VOHPO_4 \cdot 0.5H_2O$ phase topotactically transforms to (020) plane of $(VO)_2P_2O_7$, which is believed to be responsible for the catalytic activity in *n*-butane oxidation [15].

XRD patterns of all the catalysts, which were prepared by calcination of the precursors at 723 K under the flow of *n*-butane/air mixture (0.75% *n*-butane in air) for the same duration are shown in Fig. 3. These materials have similar patterns to a well-crystallized $(VO)_2P_2O_7$, with main peaks appearing at 2θ = 22.9, 28.4 and 29.38°, which correspond to (020), (204) and (221) planes, respectively.

The XRD patterns of VPO catalysts prepared with microwave irradiation method appears to be different from

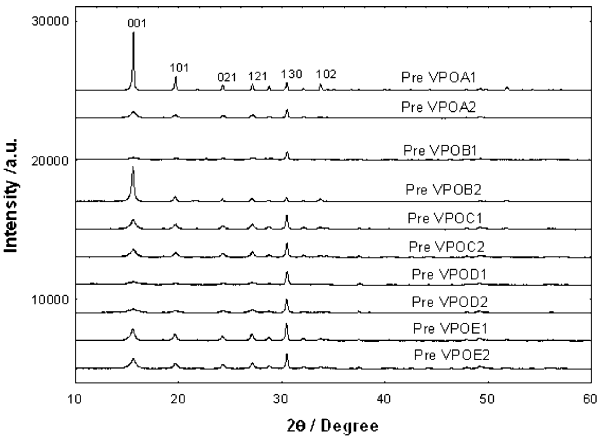

Fig. 2 XRD Patterns of microwave and conventional heated VOHPO4 · $0.5H_2O$ precursors

that of the conventionally prepared ones. Thus, we can summaries the significant differences found between catalysts prepared by the two different methods:

Increase crystallizes structure, which indicated by the higher intensity of the peaks (001) for $VOPO_4 \cdot 2H_2O$ prepared with microwave method. The vanadyl phosphate hydrate and vanadyl hydrogen phosphate hydrate, has a strong dipolar character, so both absorbed the irradiation. This dielectric heating effect lies in the capacity of an electrical field to polarize charges in a material. However, when the vanadyl phosphate hydrate and vanadyl hydrogen phosphate hydrate were heated by conventional heating, moisture is initially removed from the external surface of the pellet. Microwave drying of VPO has shown that when a wet body is exposed to microwave radiation the section that has the highest moisture content absorbs the microwave most strongly and therefore becomes the hottest part of the body. Hence, the rate of evaporation is the greatest from the wettest region.

The particle thickness for all VPO catalysts at (020) and (204) were given by the Debye–Scherrer equation [16]

$$t = \frac{0.89\lambda}{\beta_{hkl}\mathrm{Cos}\theta_{hkl}}$$

where t is the particle thickness for (*hkl*) phase, λ is the X-ray wavelength of radiation for CuK_α, β_{hkl} is the full width at half maximum (FWHM) at (*hkl*) peak in radian and θ_{hkl} is the diffraction angle for (*hkl*) phase. The parameter used to determine the crystal size of the catalysts is the half width of the (020) reflection. The line width increases with the decreasing of the crystallites size. The decrease of the FWHMs of the (020) reflection indicates that the particle thickness in the (020) direction increases. In the experiments using large crystallites

of $(VO)_2P_2O_7$, the surface which is selective for the formation of maleic anhydride is the (020) plane, and the side faces such as (001) are active for nonselective oxidation. Thickness of (204) plane is only indicative of the mean "length" at (204) face, while the thickness of (020) is more representative of the actual thickness [17]. Table 2 shows the line width of the (020) and (204) plane reflections. The particle thickness at (020) plane for the catalyst, which prepared via microwave heating is generally smaller compared with the catalyst prepared via conventional heating, except for the VPOC2 and VPOD2. Furthermore, the particle thickness of (204) planes for all catalyst prepared by microwave heating also smaller compared to the catalyst prepared by conventional heating, except for the VPOE2. A smaller particle size at (020) plane may enhanced the selectivity of the catalyst. The exposure of (020) plane would a great significance in improvement of the catalytic performance of vanadium phosphate catalyst [18].

3.2 BET Surface Area Measurement and Redox Titration

The specific surface area of all microwave heated catalysts (Tables 1, 2) is shown to be larger than those under conventional heating. The mechanics of heat diffusing in the conventional heating process was that heat gradually diffused from outer to inner. Gas and liquid coexist in the pore of the gel and form a meniscus following solvent evaporation. The meniscus gradually shrunk into the pore for the effect of surface tension. The capillary force drew the pore framework and made it breakdown accompany with the temperature, and then the specific surface area and volume of the catalysts became very little [19]. However, the mechanics of heat generation in the microwave irradiation, the energy transfer to inside complex and heat produce from interaction of irradiation with polar bond in complex. When a wet body is exposed to microwave radiation the section that has the highest moisture content absorbs the microwave

Table 1 Preparation condition and specific surface area of the catalysts

Catalysts	Molar ratio	Preparation condition	Heating	BET (m^2g^{-1})
VPOA1	P:V = 1.1:1	VPOH1($VOPO_4 \cdot 2H_2O$) + iso-butanol	Microwave	24
VPOA2	P:V = 1.1:1	VPOH2($VOPO_4 \cdot 2H_2O$) + iso-butanol	Conventional	21
VPOB1	P:V:Nb = 1.1:1:0.04	VPOH1($VOPO_4 \cdot 2H_2O$) + iso-butanol + Nb_2O_5	Microwave	34
VPOB2	P:V:Nb = 1.1:1:0.04	VPOH2($VOPO_4 \cdot 2H_2O$) + iso-butanol + Nb_2O_5	Conventional	21
VPOC1	P:V:Mo = 1.1:1:0.01	VPOH1($VOPO_4 \cdot 2H_2O$) + iso-butanol + $((NH_4)_6Mo_7O_{24}) \cdot 4H_2O$	Microwave	17
VPOC2	P:V:Mo = 1.1:1:0.01	VPOH2($VOPO_4 \cdot 2H_2O$) + iso-butanol + $((NH_4)_6Mo_7O_{24}) \cdot 4H_2O$	Conventional	16
VPOD1	P:V:Co = 1.1:1:0.01	VPOH1($VOPO_4 \cdot 2H_2O$) + iso-butanol + $CoN_2O_6 \cdot 6H_2O$	Microwave	20
VPOD2	P:V:Co = 1.1:1:0.01	VPOH2($VOPO_4 \cdot 2H_2O$) + iso-butanol + $CoN_2O_6 \cdot 6H_2O$	Conventional	15
VPOE1	P:V:Bi = 1.1:1:0.01	VPOH1($VOPO_4 \cdot 2H_2O$) + iso-butanol + Bi $(No_3)_3 \cdot 5H_2O$	Microwave	21
VPOE2	P:V:Bi = 1.1:1:0.01	VPOH2($VOPO_4 \cdot 2H_2O$) + iso-butanol + Bi $(No_3)_3 \cdot 5H_2O$	Conventional	20

Table 2 XRD data of undoped and doped VPO catalysts prepared via MW and CH

Catalysts	Line width[a] (020)/Å	Line width[b] (204)/Å	Thickness[c] (020)/Å	Thickness[c] (204)/Å
VPOA1	0.5749	0.455	139.39	178.04
VPOA2	0.3466	0.4253	231.08	190.46
VPOB1	0.44	0.4968	181.83	163.07
VPOB2	0.264	0.3125	303.54	259.22
VPOC1	0.8557	0.6606	93.64	122.65
VPOC2	0.9083	0.4303	88.18	188.2
VPOD1	1.1244	0.3869	71.25	209.39
VPOD2	1.1934	0.3844	67.15	210.76
VPOE1	0.79	0.4008	101.38	202.01
VPOE2	0.7176	0.4221	111.61	191.83

[a] FWHM of (020) reflection

[b] FWHM of (204) reflection

[c] Plate thickness by means of Scherrer's formula: $T(Å) = (0.89 \times \lambda)/(FWHM \times \cos\theta)$

Table 3 Average oxidation numbers and percentages of V^{5+} and V^{4+} oxidation states present in catalysts prepared via MW and CH

Catalyst	V^{5+}(%)	V^{4+}(%)	Ave. oxdn. no.
VPOA1	30	70	4.30
VPOA2	26	74	4.26
VPOB1	28	72	4.28
VPOB2	27	73	4.27
VPOC1	23	77	4.23
VPOC2	18	82	4.18
VPOD1	18	82	4.18
VPOD2	16	84	4.16
VPOE1	17	83	4.17
VPOE2	21	79	4.21

most strongly and therefore becomes the hottest part of the body. Hence, the rate of evaporation is the greatest from the wettest region. This effect change in morphology, pore value and pore size. Surface tension and capillary force would disappear because the outer and inner of catalyst was heat simultaneously when it was dried by microwave. It would prevent the collapse of the gel and the framework (three-dimensional net structure) of it could be preserved. Then the specific area and pore volume of the catalysts were larger.

The average oxidation number and percentage of V^{5+} and V^{4+} oxidation states are shown in Tables 3, 4 For all catalysts (undoped and doped), microwave irradiation increases the average oxidation number by induced the presence of higher amount of V^{5+} phase except for Bi doped catalyst.

Table 4 Total amounts of oxygen atoms removed and ratio for oxygen removed of V^{5+}/V^{4+} obtained by temperature programmed reduction in H_2/Ar (H_2–TPR)

Catalysts	Peak	T_{max}(K)	Oxygen atoms removed (mol g^{-1}) × 10^{-4}	Oxygen atoms removed (atom g^{-1}) × 10^{21}	Ratio for oxygen removed of V^{5+}/V^{4+}
VPOA1	1	804	6.14	0.37	0.38
	2	1056	1.6	0.97	
Total oxygen atoms removed			2.21	1.34	
VPOA2	1	778	3.65	0.22	0.25
	2	1044	1.46	0.88	
Total oxygen atoms removed			1.82	1.1	
VPOB1	1	903	2	1.21	0.22
	2	1122	9.34	5.63	
Total oxygen atoms removed			11.34	6.84	
VPOB2	1	887	1.29	0.78	0.25
	2	1081	5.55	3.34	
Total oxygen atoms removed			6.84	4.12	
VPOC1	1	843	0.74	0.45	0.47
	2	1040	1.57	0.95	
Total oxygen atoms removed			2.31	1.4	
VPOC2	1	796	0.08	0.05	0.05
	2	992	1.85	1.11	
Total oxygen atoms removed			1.93	1.16	
VPOD1	1	941	0.48	0.29	0.16
	2	1058	3.05	1.84	
Total oxygen atoms removed			3.53	2.13	
VPOD2	1	756	0.63	0.04	0.04
	2	1048	1.63	0.98	
Total oxygen atoms removed			1.69	1.02	
VPOE1	1	886	0.15	0.09	0.07
	2	908	2.12	1.28	
Total oxygen atoms removed			2.27	1.37	
VPOE2	1	847	0.75	0.45	1.1
	2	911	0.68	0.41	
Total oxygen atoms removed			1.43	0.86	

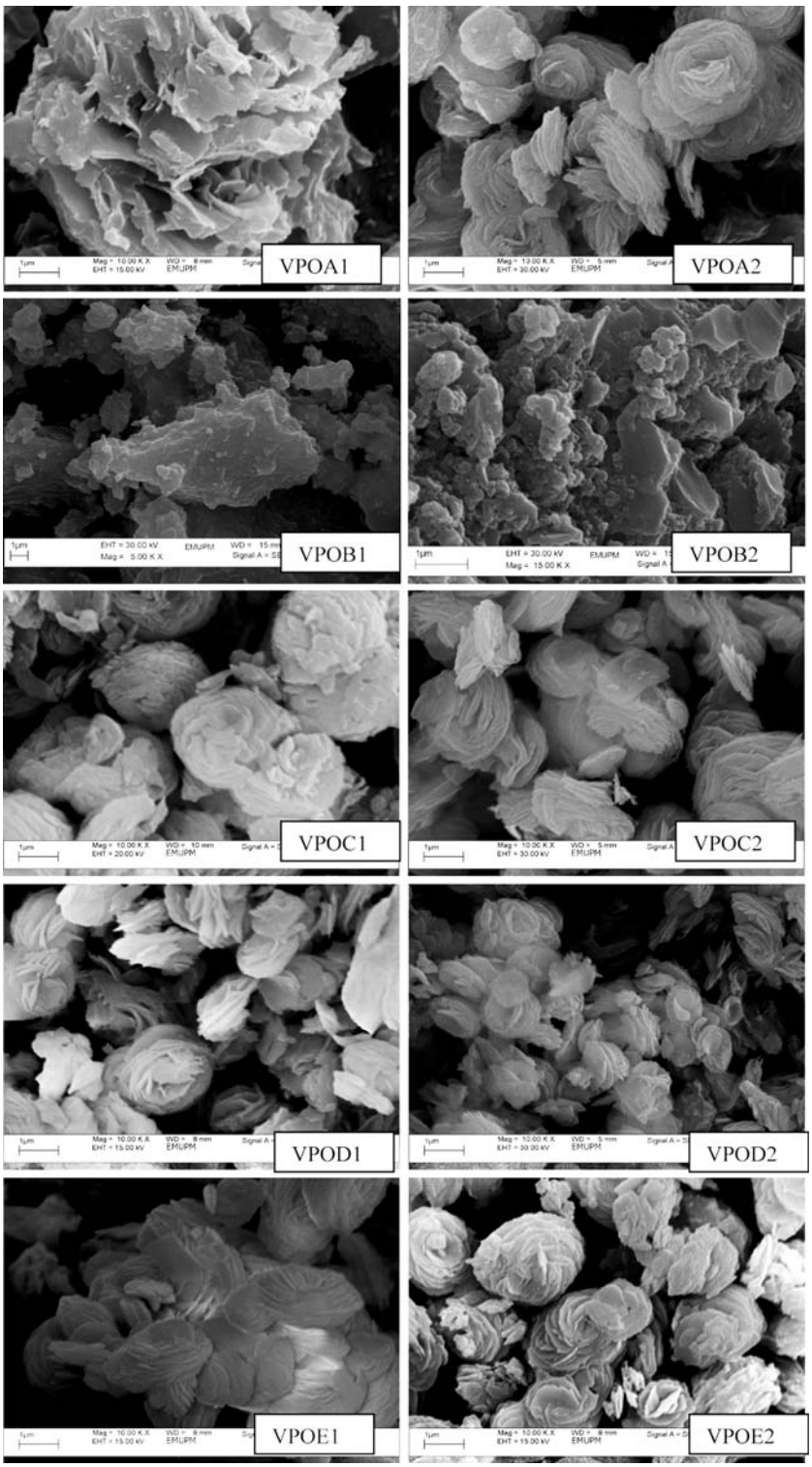

Fig. 4 Scanning electron micrographs of microwave and conventional heated catalysts

3.3 Scanning Electron Microscopy (SEM)

The surface morphology of the materials was examined using scanning electron microscopy (Fig. 4). The principle structure of all the catalysts is the same, consisting of rosette plate like crystals (except for Nb doped catalyst which is bulky and irregular shape). However the microwave irradiated catalysts shown a thinner rosette-type structure with a crystallite of uniform size.

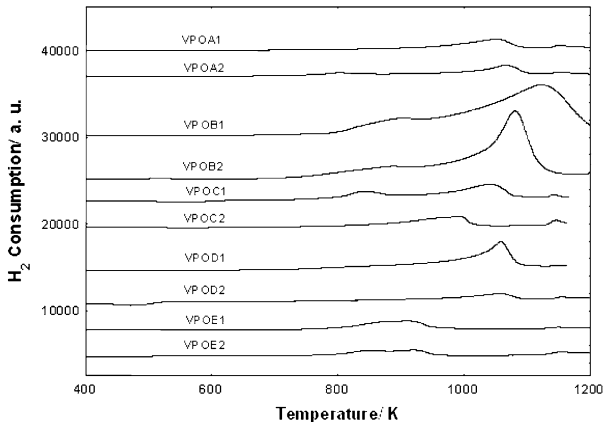

Fig. 5 TPR Profiles of $(VO)_2P_2O_7$ catalysts prepared by microwave and conventional heating

3.4 Temperature Programmed Reduction (TPR) in H_2/Ar

Figure 5 shows the TPR profiles of all the catalysts. Two reduction peaks are observed in the rate of H_2 consumption which the lower peak is corresponding to the reduction of V^{5+} phase whereas the second reduction peak occurred at higher temperature is correspond to the reduction of V^{4+} phase. These two reduction peaks observed for microwave-heated catalysts were slightly shifted to higher temperature than the conventional heated catalyst. However, interestingly the total amount of the oxygen species removed from the microwave-heated catalyst is much higher. Electrical conductivity investigation on this catalyst suggested that O^{2-} is associated with V^{5+} phase whereas O^- is associated with V^{4+} phase [20]. A good direct correlation was reported [21] between the amount of oxygen species removed from both phases (V^{4+} and V^{5+}) with the *n*-butane conversion and MA selectivity, respectively. Therefore, a higher amount of oxygen removed from microwave-heated catalyst suggested that microwave process is capable and potential to produce highly reactive and selective oxygen species for butane oxidation to MA.

3.5 Oxidation of n-Butane to Maleic Anhydride

(1.7% n-butane in air, GHSV: 2400 h^{-1}, 673 K)

A significant improvement of the catalytic performance is observed for the *n*-butane conversion and for the selectivity of MA when the VPO catalyst was irradiated with microwave. VPOB1 gave 74% of conversion (three fold) compared to only 25% for conventional heated catalyst (VPOB2) whereas the MA selectivity was increased from 56% (VPOB2) to 60% for microwave-irradiated catalyst (VPOB1) (Table 5). This effect can be correlated with the increase of the BET area which connected to the development of (020) plane of $(VO)_2P_2O_7$. Microwave irradiation also leads to the reducibly behavior of the catalyst. Higher amount of active site (V^{4+}) and oxygen species, which responsible for activation of *n*-butane also contributed to the enhancement of the activity. Furthermore, the smaller particle size at (020) plane obtained for the microwave irradiated catalyst, which tends contributed strongly to improved the MA selectivity.

Table 5 Catalytic performance of VPOB1 and VPOB2 for the oxidation of *n*-butane to maleic anhydride[a]

Catalyst	*n*-Butane conversion (%)	Selectivity (%)		
		MA	CO	CO_2
Microwave (VPOB1)	74	60	28	11
Conventional (VPOB2)	25	56	32	12

[a] Reaction condition: 673 K, 1.7% *n*-butane in air, GHSV: 2400 h^{-1}

4 Conclusion

In this present study we have shown for the first time the microwave irradiation used to prepared VPO catalyst via dihydrate route. The microwave irradiation induced a higher crystallinity of vanadyl phosphate hydrate and vanadyl hemihydrates precursor compared to the conventional heated catalyst. Our present results therefore provide a novel approach to obtain mesostructured VPO compounds and this affected the surface area and catalytic property for selective oxidation of *n*-butane to maleic anhydride. Microwave irradiation enhanced both the activity and selectivity of VPO catalyst by induced the mobility and availability of the O^- and O^{2-} surface ions. Furthermore, it also reduced the particle size of (020) plane, which improved the MA selectivity.

Acknowledgement Financial assistance from Malaysian Ministry of Science, Technology and Innovation (MOSTI) is gratefully acknowledged.

References

1. Griesel L, Bartley JK, Wells RPK, Hutchings GJ (2003) Catal Today 81:197
2. Cavani F, Trifirò F (1995) Stud Surf Sci Catal 91:1
3. Hutchings GJ, Desmartin Chomel A, Olier R, Volta JC (1994) Nature 368:41
4. Hutchings GJ (2004) J Mater Chem 14:3385
5. Kiely CJ, Burrows A, Hutchings GJ, Bere KE, Volta JC, Tuel A, Abon M (1996) J Chem Soc, Faraday Discuss 105:103
6. Johnson JW, Johnston DC, Jacobson AJ, Brody JF (1984) J Am Chem Soc 106:8123
7. Ait-Lachgar K, Abon M, Volta JC (1991) J Catal 171:383
8. Lombardo EA, Sanchez CA, Conaglia LM (1992) Catal Today 15:407

9. Ben Abdelouahab F, Volta JC, Olier R (1994) J Catal 148:334
10. Ellison IJ, Hutchings GJ, Sananes M T, Volta J C (1994) J Chem Soc, Chem Commun 1093
11. Kiely CJ, Burrows A, Sajip S, Hutchings GJ, Sananes MT, Tuel A, Volta JC (1996) J Catal 162:31
12. Dagani R (1997) Chem Eng News 75:26
13. Roussy G, Thiebaut JM, Souiri M, Marchal E, Kiennemann A (1994) Catal Today 21:349
14. Niwa M, Murakami Y (1982) J Catal 76:9
15. Haber J, Zazhigalov VA, Stoch J, Bogutskaya LV, Batcherikova IV (1997) Catal Today 33:39
16. Klug PH, Alexander LE (1974) John Wiley and Sons, New York, pp 618
17. Kesteman E, Merzouk M, Taouk B, Borders E, Contractor R (1995) Systematic control of crystal morphology during preparation of selective vanadyl pyrophosphate. In: Poncelet G, Martens J, Delman B, Jacobs PA, Grange P (eds) Preparation of catalysis VI. Elsevier Science BV, Amsterdam, 707–716
18. Igarashi H, Tsuji K, Okuhara T, Misono M (1993) J Phys Chem 97:7065
19. Zeng L, Jiang H, Niu J (2005) J Mol Catal A: Chem 232:119
20. Abon M, Herrmann J, Mand Volta JC (2001) Catal Today 71:121
21. Taufiq-Yap YH, Goh CK, Hutchings GJ, Dummer N, Bartley JK (2006) J Mol Catal A: Chem 260:24